

USE OF EMBEDDED CORROSION SENSORS AND SENSOR BLANKETS TO DETECT PAINT DEGRADATION

G.D. Davis and C.M. Dacres
DACCO SCI, INC.
10260 Old Columbia Road
Columbia, MD 21046
davis@daccosci.com

ABSTRACT

In-situ corrosion sensors based on electrochemical impedance spectroscopy (EIS) have been used to detect coating defects and monitor coating degradation. Three versions of the sensor were evaluated: sensors embedded between the primer and topcoat, sensors permanently attached to the topcoat surface, and sensors mounted on the surface only during the measurement process. Each version offers potential to localize coating defects with the portability of the third version (sensor blanket) providing advantages in inspecting existing structures.

Keywords: sensor, electrochemical impedance, corrosion, coating, degradation, health monitoring

INTRODUCTION

Undetected corrosion can impact safety and readiness of critical equipment and structures. In extreme cases, it can cause catastrophic failure with fatalities. The most common corrosion protection scheme uses paints and other coatings. However, as coatings degrade or become damaged, they lose their protective ability. For critical applications, condition-based maintenance (CBM) is needed to prevent structural damage as the coating degrades. One means by which health monitoring of coatings can be achieved is with the use of corrosion sensors. *In-situ* corrosion sensors based on electrochemical impedance spectroscopy (EIS) have been previously reported.¹⁻⁵ EIS is an established laboratory technique for investigating coating deterioration and substrate corrosion during immersion in an electrolyte,⁶⁻¹⁰ but could not previously be used in ambient or service conditions. The *in-situ* corrosion sensors permit EIS measurements in such conditions. They directly inspect the coating and underlying structures, as opposed to corrosivity sensors that simply monitor the environment. Consequently, the technology is ideally suited for health monitoring.

Two approaches for health monitoring are discussed here: a smart coating with one or more embedded sensors and a sensor blanket with one or more sensor electrodes. A smart coating is well suited for remote monitoring of critical structures. With suitable electronics, monitoring can occur from a central location. The sensor blanket will allow inspection of multiple structures and localization of coating defects and substrate corrosion. Both approaches enable condition-based maintenance of critical structures and equipment.

EXPERIMENTAL PROCEDURE

Steel 6"x4" (150mm x 100mm) test panels were painted with a household metal primer and enamel topcoat. (These coatings were chosen as ones that would likely degrade in a relatively short test program so that the effectiveness of the sensor concepts could be demonstrated. It is expected that the technology will be directly applicable to other primers and topcoats.) Two sensor electrodes were applied to the primer surface using a conductive adhesive film. Wires were connected to the electrodes and to the back surface; the connections were sealed with epoxy prior to applying the topcoat. For some specimens, a small area was masked so that it received no primer to represent a coating defect. All panels received a topcoat. Some panels were then scribed through the

topcoat and primer for another coating defect. This defect was approximately in the same location as the primer defect. Additional panels were nominally defect-free. Exterior electrodes were then applied to the topcoat surface of half of the specimens.

EIS measurements were taken with each sensor both before salt fog exposure and following various periods of salt fog exposure without removing the specimens from the chamber, i.e., the electrode connection wires were snaked outside of the chamber so that a commercial potentiostat could interrogate each sensor, in turn. Impedance spectra were modeled with the equivalent circuit shown in Figure 1. This circuit has previously been used for coated specimens and adhesive bonds with good success. It provided excellent fits to the data.

Larger 12"x6" (300mm x 150mm) panels were also prepared with a topcoat defect to evaluate the sensor array approach. Additional measurements were made on an e-coated trunk lid. Sensor arrays with different electrode sizes and configurations were fabricated to develop procedures to locate coating defects. Surface conductivity of the topcoat was adjusted by water spraying and ultrasonic couplant brushing. EIS measurements were obtained as a function of electrode distance from the defect. Although the circuit of Figure 1 gave reasonable fits to the data, improved fits were obtained using the circuit of Figure 2. Low-frequency impedance, a much simpler parameter, was also used to describe the data.

RESULTS AND DISCUSSION

Figure 3 shows examples of the EIS spectra from one of the specimens with the primer defect. The particular sensor indicated is the internal sensor away from the defect. Initially the coating exhibits a ca-

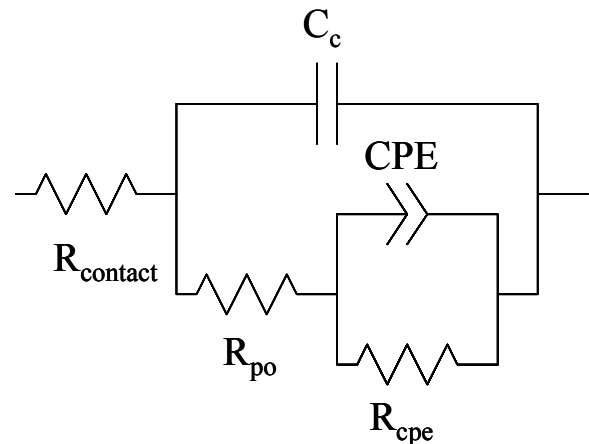


Figure 1. Circuit used for embedded and surface-mounted sensors.

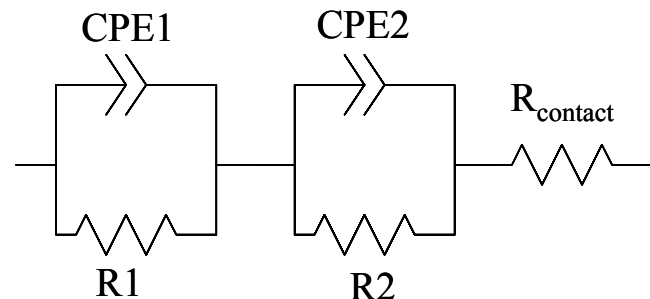


Figure 2. Equivalent circuit used for contact sensors for defect localization.

capacitive behavior with a very high low-frequency impedance. As degradation begins, the low-frequency region becomes resistive (independent of frequency).

The low-frequency impedance is shown for each of the sensors on the specimens with defects in the primer and in the topcoat (Figure 4). There was a small decrease in the low-frequency impedance for the primer defect specimen upon exposure, especially for the two sensors away from the defect because they had the higher initial impedance. The impedance remained constant until the 28-day measurements, at which point they dropped substantially. This delay likely represents the time required for the topcoat to absorb moisture and degrade.

In the case of the topcoat-defect specimens, the sensors closest to the defect detect the defect immediately with a significant drop in impedance at the first measurement following exposure. The farther sensors take a longer time to detect the defect (based on low-frequency impedance). This time is similar to the incubation time seen with the primer-defect specimens, which is consistent with a moisture absorption process that increases the conductivity of the topcoat. One important observation from these measurements is that for this type of defect, the internal and external sensors appear equally effective.

The nominally defect-free specimens are interesting in that unintentional defects are readily seen on one of the specimens as shown in Figure 5. For the panel on the left, a gradual decrease in low-frequency impedance, typical of coating degradation, is seen in the nearly three months of exposure. No defects are indicated. For the panel on the right, an immediate decrease in impedance is seen for three of the sensors indicating at least one unintentional defect near #2 sensors. After the first measurement following exposure, suspected areas were touched up with topcoat; however, at least some defects were in other locations as detected by the sensors.

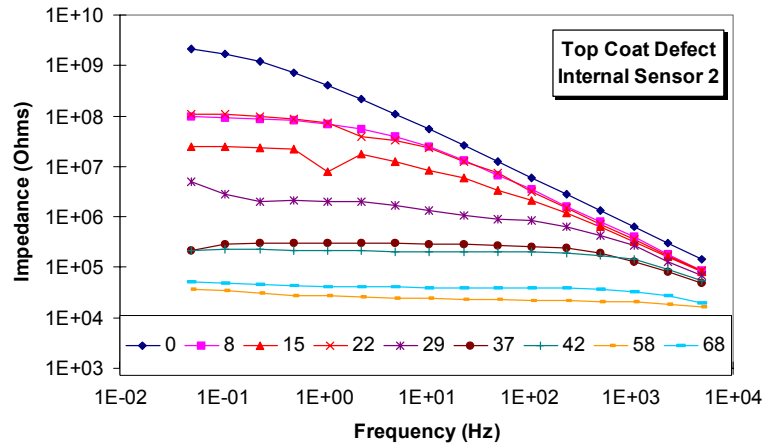


Figure 3. Impedance spectra (Bode magnitude plots) of the second internal sensor of one of the top coat defect specimens. The legend gives the exposure period in days.

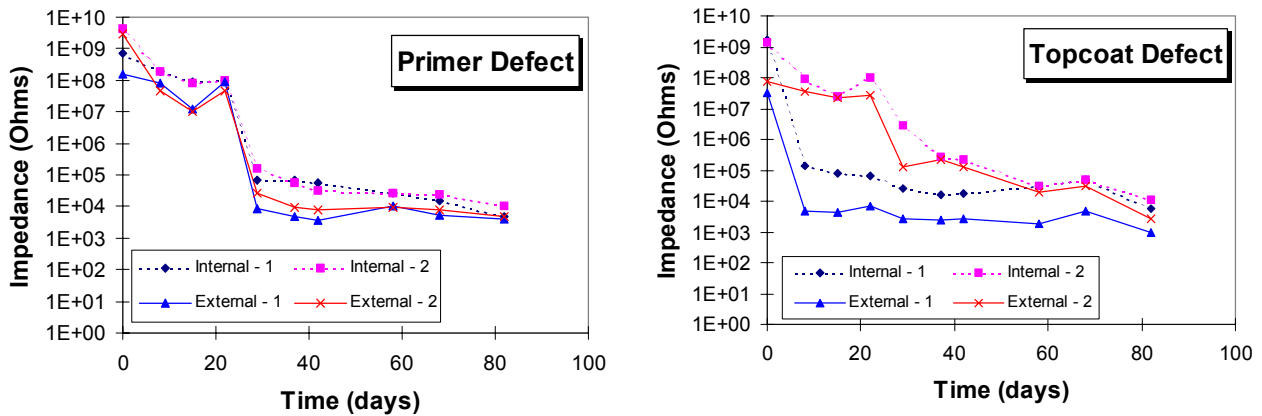


Figure 4. Low-frequency impedance as a function of salt fog exposure for the primer defect specimen (left) and topcoat defect specimen (right). The #1 sensors are close to the defect; the #2 sensors are farther away.

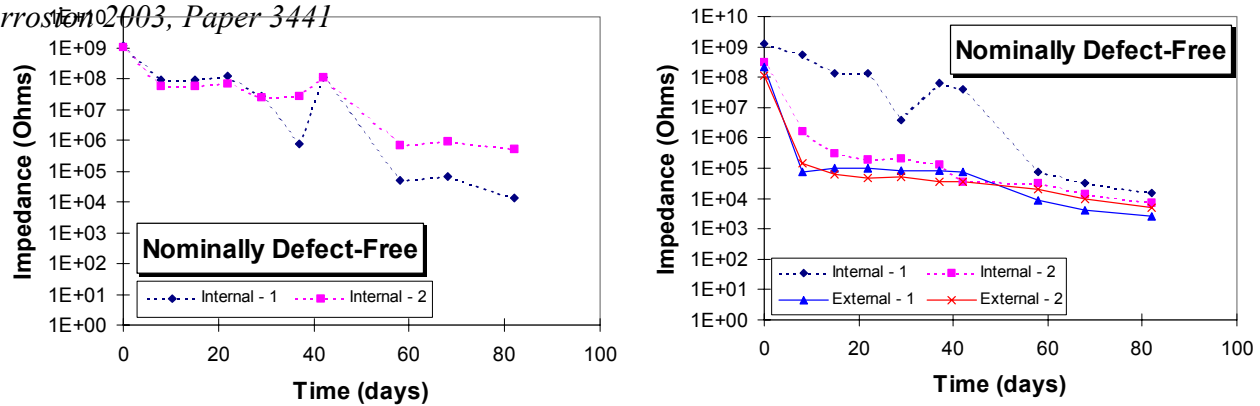


Figure 5. Low-frequency impedance for the two nominally defect-free specimens.

These data were also modeled with the equivalent circuit shown in Figure 1. Examples of some of the circuit parameters as a function of time for the different sensors are given in Figure 6. Both of these circuit parameters (CPE and R_{cpe}) vary by up to five orders of magnitude as the coating defect allows attack of the specimen. These data show that the two pairs of external and internal sensors track very well, indicating that either approach is suitable. On the other hand, there is a distinct difference between the sensors closer to the defect and those farther away from the topcoat defect, indicating the potential to localize coating defects.

The sensor blanket concept was initially evaluated using a metal mesh or screen electrode blanket consisted of a single screen segment. This blanket was tested on the small painted panels with the embed-

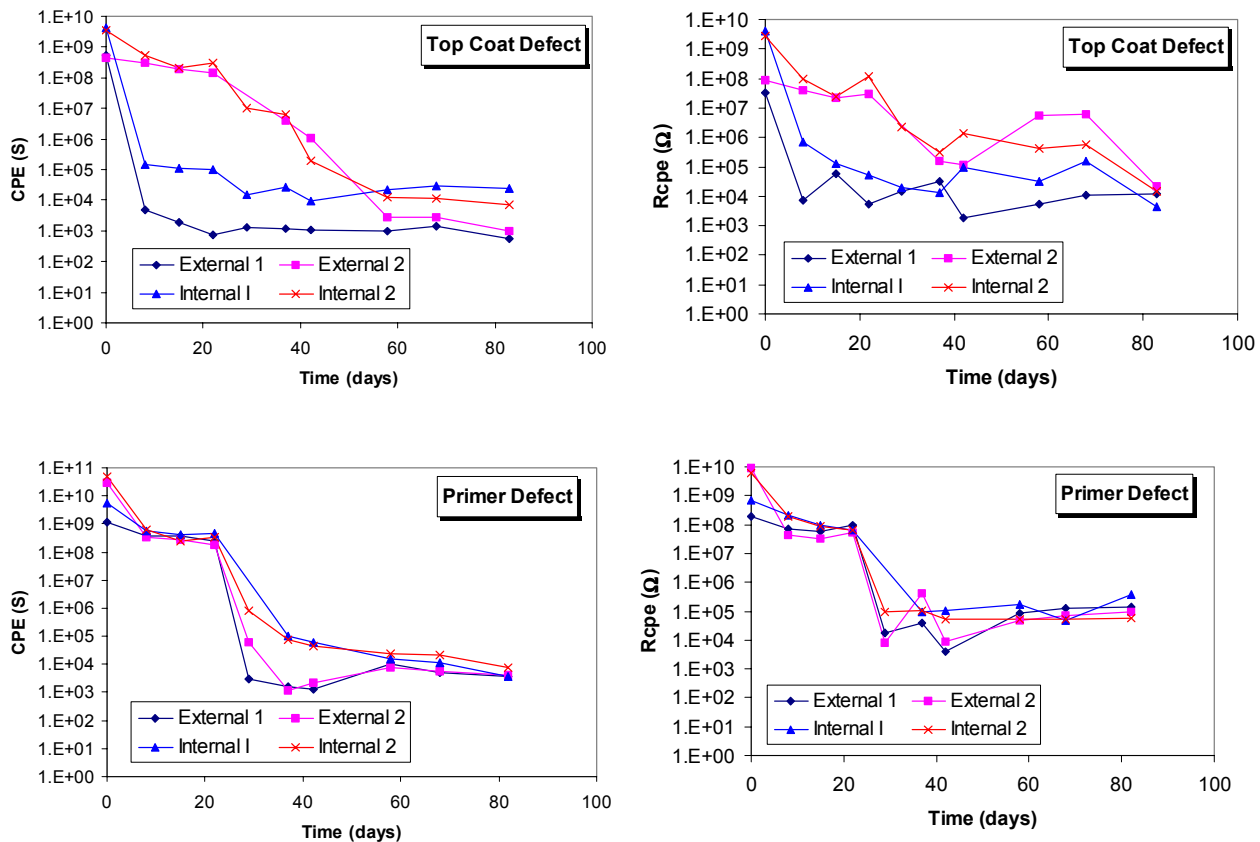


Figure 6. Equivalent circuit parameters for the top coat-defect specimen and the primer-defect specimen.

ded sensors (without the topcoat sensors). Measurements were taken on both the unexposed, reserve panels and the panels exposed to salt fog for 4 months. Both low-frequency impedance measurements and equivalent circuit modeling were performed using the circuit of Figure 2.

The results are shown in Figure 7. The sensor blanket clearly shows the presence of both the primer defect and the topcoat defect before exposure to salt fog. The primer defect, the more subtle of the defects to detect, caused a decrease of at least a factor of 30 in the low-frequency impedance and in each circuit parameter shown. The decrease for the topcoat defect is much greater, as expected. Following salt fog exposure, all specimens exhibit very low sensor values as the coating has degraded to allow exposure of the substrate. Thus, the signals are very similar to that of the initial topcoat defect. Although equivalent circuit modeling may ultimately prove useful in distinguishing coating degradation and different types of defects, these initial results suggest that the simpler low-frequency impedance is sufficient to at least alert an inspector to a coating problem.

By using arrays of smaller sections of metal mesh, localization of coating defects can be achieved by interrogating individual mesh sections. This was demonstrated by dividing the mesh into four sections to form a quadrant blanket. The results are illustrated in Figure 8. The ultrasonic couplant was brushed on the blanket electrodes to improve conductivity. The A-sensor was placed on top of the topcoat defect of the unexposed large panel. A clear difference of two orders of magnitude or more is seen in the low-frequency impedance, sum of the resistances and sum of the constant phase elements. Such results demonstrate the feasibility of this type of blanket. The measurements were repeated using water instead of the ultrasonic couplant. Similar results were obtained although the difference between the “A” sensor and the other sensors was less.

Additional measurements were made on an e-coated trunk lid on which a small scribed coating defect

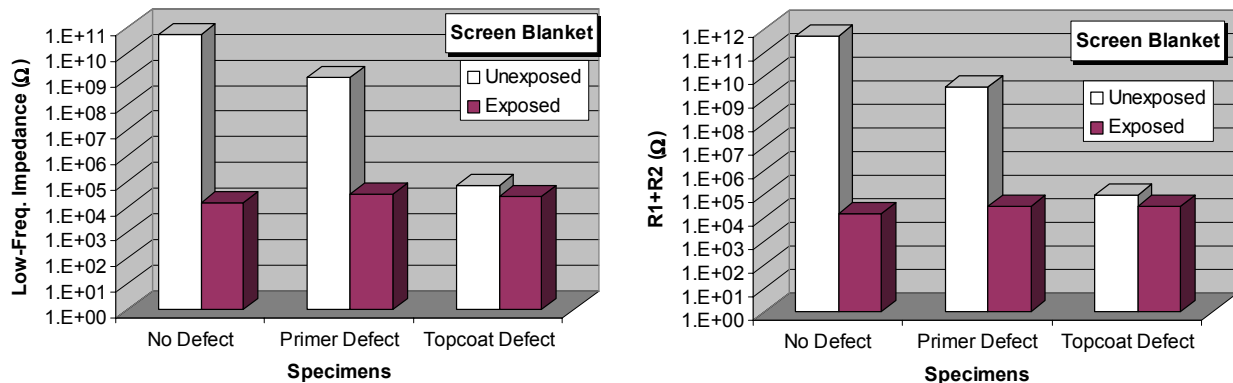
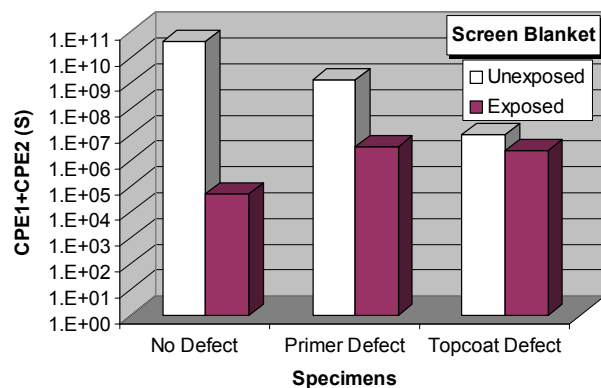


Figure 7. Results from the screen electrode blanket (single sensor) inspecting painted panels with no defect, primer defect, and topcoat defect before and after 4-months salt fog exposure.



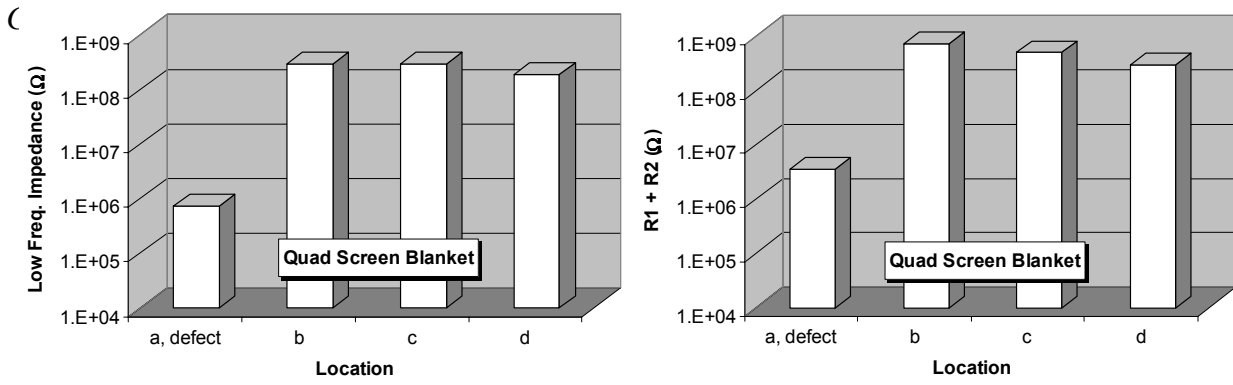
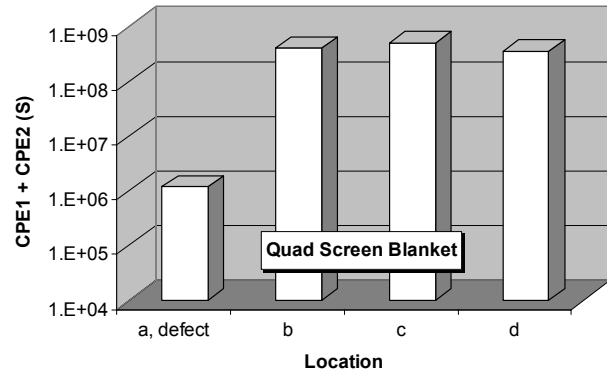


Figure 8. Sensor signals from each of quadrant of the four-mesh blanket. The A-quadrant mesh sensor was placed over a topcoat defect.



was introduced. These results are given in Figure 9. They clearly exhibit the same behavior as the large

panel with the quadrant with the defect (“A” sensor) easily indicating the defect. Measurements were also taken by electrically connecting all the mesh electrodes together. The combined measurements were similar to the measurements with the “A” sensor. Thus, a global inspection of a structure can be made with all the electrodes connected. If a defect is indicated, different combinations of the electrodes can be interrogated sequentially until the defect(s) are localized. This has the potential of reducing in-

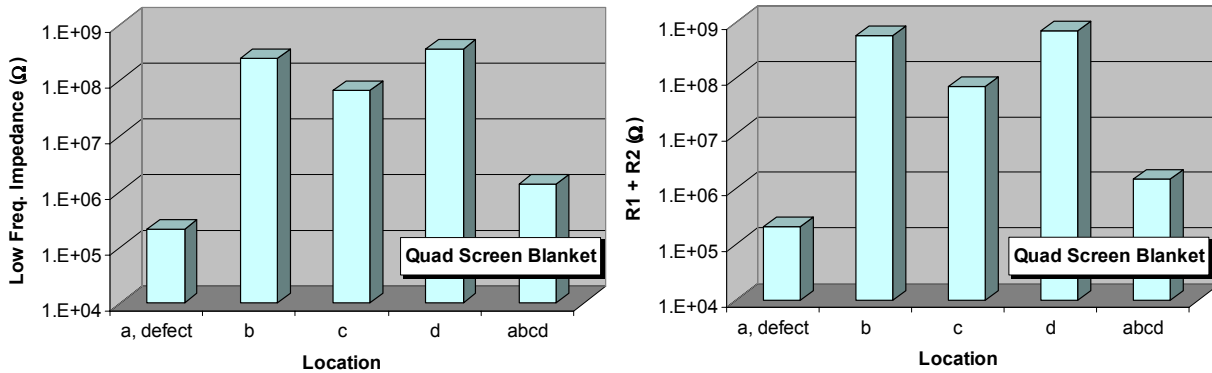
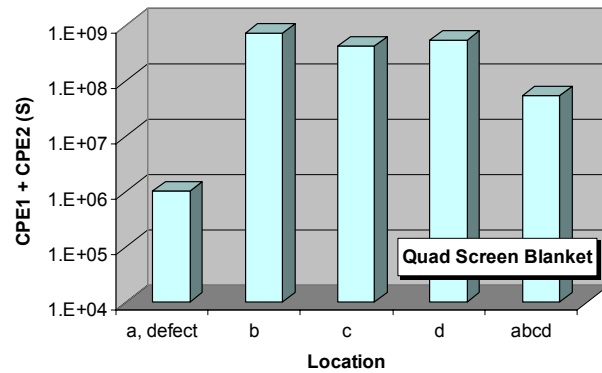


Figure 9. Sensor signals from each of quadrant of the four-mesh blanket on the trunk lid with a scribed coating defect. The A-quadrant mesh sensor was placed over a coating defect. The abcd reading involved coupling the four quadrants together as an overall measurement.



spection time by quickly indicating good areas.

CONCLUSIONS

Both embedded and external sensors are capable of detecting coating defects and degradation. Coating defects can be located by the use of arrays of metal mesh electrodes.

ACKNOWLEDGEMENTS

We gratefully acknowledge the technical assistance of Fernando Garra. This work was funded by the Army Corps of Engineers Construction Research Engineering Laboratory (CERL) under contract DACA42-02-C-0035.

REFERENCES

1. G.D. Davis and C.M. Dacres, “Electrochemical Sensors for Evaluating Corrosion and Adhesion on Painted Metal Structures,” U.S. Patent 5,859,537; “Portable Hand-Held In-Situ Electrochemical Sensor for Evaluating Corrosion and Adhesion on Coated and Uncoated Metal Substrates,” U.S. Patent 6,054,038; “In-Situ Electrochemical-Based Moisture Sensor for Detecting Moisture in Composite and

Bonded Structures,” U.S. Patent 6,313,646; “An Adhesive Tape Sensor for Detecting and Evaluating Coating and Substrate Degradation Utilizing Electrochemical Processes,” U.S. Patent 6,328,878.

2. G.D. Davis, C.M. Dacres, and L.A. Krebs, “EIS-Based *In-Situ* Sensor for the Early Detection of Coating Degradation and Substrate Corrosion,” *Corrosion2000*, Paper 275 (NACE, Houston, TX, 2000).
3. G.D. Davis, C.M. Dacres, and L.A. Krebs, *Materials Performance* **39**, 46 (2000).
4. L.A. Krebs, G.D. Davis, and C.M. Dacres, “Monitoring Moisture Intrusion and Coating Degradation in the Field,” *Corrosion2001*, Paper 1430 (NACE, Houston, TX, 2001).
5. G.D. Davis, L.A. Krebs, and C.M. Dacres, “Coating Evaluation and Validation of Accelerated Test Conditions Using an *In-Situ* Corrosion Sensor,” *J. Coatings Technol.* **74**(935), December 2002.
6. J.R. Scully, *J. Electrochem. Soc.* **136**, 979 (1989).
7. W.S. Tait, *J. Coat. Technol.* **61**, 57 (1989).
8. J.R. Scully, in *Corrosion Testing and Evaluation: Silver Anniversary Volume, ASTM STP 1000*, R. Baboian and S.W. Dean, eds., (American Society for Testing and Materials, Philadelphia, 1990), p. 351.
9. J.N. Murray and H.P. Hack, *Corrosion90*, Paper 140, NACE, Houston, TX, 1990.
10. F. Mansfeld, M.W. Kendig, and S. Tsai, *Corrosion* **38**, 478 (1982).